Large-gap Peripheral Nerve Repair Using Xenogeneic Transplants in Rhesus Macaques

Paul Holzer (pholzer1@jhu.edu)
Whiting School of Engineering, Johns Hopkins University, Baltimore, Maryland
Elizabeth J. Chang
XenoTherapeutics Inc., 501(c)3, Boston, Massachusetts
Jamie Tarlton
Department of Biological and Biomedical Sciences, Glasgow Caledonian University, Glasgow
Diana Lu
XenoTherapeutics Inc., 501(c)3, Boston, Massachusetts
Natasha Gillespie
Department of Biological and Biomedical Sciences, Glasgow Caledonian University, Glasgow
Kaitlyn Rogers
XenoTherapeutics Inc., 501(c)3, Boston, Massachusetts
Jon Adkins
XenoTherapeutics Inc., 501(c)3, Boston, Massachusetts
Monica Metea
Preclinical Electrophysiology Consulting, LLC, Boston, Massachusetts
Alan LaRochelle
Biomedical Research Models, Inc. (Biomere), Worcester, Massachusetts
Joan Wicks
StageBio, Mt Jackson, Virginia
Buket Onel
Xeno Diagnostics, LLC, Indianapolis, Indiana
Steve Gullans
XenoTherapeutics Inc., 501(c)3, Boston, Massachusetts
Joshua C. Doloff
Department of Biomedical Engineering, Translational Tissue Engineering Center, Johns Hopkins University School of Medicine, Baltimore, Maryland
Linda Scobie
Department of Biological and Biomedical Sciences, Glasgow Caledonian University, Glasgow
Curtis L. Cetrulo, Jr.
Reconstructive Transplantation Laboratory, Massachusetts General Hospital, Boston, Massachusetts
Rod Monroy
XenoTherapeutics Inc., 501(c)3, Boston, Massachusetts

Research Article

Keywords:

Posted Date: February 28th, 2022

DOI: https://doi.org/10.21203/rs.3.rs-846240/v2

Abstract

Surgical intervention is required to successfully treat severe, large-gap (≥4 cm) peripheral nerve injuries. However, all existing treatments have shortcomings and an alternative to the use of autologous nerves is needed. Human andporcine nerves are physiologically similar, with comparable dimensions and architecture, presence and distribution of Schwann cells, and conserved features of the extracellular matrix (ECM). We report the repair of fully transected radial nerves in 10 Rhesus Macaques using viable, whole sciatic nerve from genetically engineered (GalT-KO), designated pathogen free (DPF) porcine donors. This resulted in the regeneration of the transected nerve, recovery of wrist extension function, distal muscle reinnervation, and recovery of nerve conduction velocities and compound muscle action potentials statistically equivalent to autologous controls. We also demonstrate the absence of immune rejection, systemic porcine cell migration, and detectable residual porcine material. Our findings support the safety and efficacy of viable porcine nerve transplants, suggest the interchangeable therapeutic use of cross-species cells, and highlight the broader clinical potential of xenotransplantation.

Introduction

Severe trauma to the extremities frequently results in neurotmesis, the complete transection of peripheral nerves, a devastating injury. [1, 2]. It is estimated that twenty million Americans suffer from peripheral nerve injury (PNI) resulting in nearly 50,000 surgeries annually [1]. Treatment of injuries 4 cm, termed large-gap PNIs, are especially challenging as direct coaptation is only possible for smaller defects [3, 4]. In such cases, a nerve conduit (NC) is needed. The use of autologous nerves, such as the sural, is considered the standard of care despite complications such as donor site morbidity, chronic pain, paraesthesia, insufficient length, or improperly matched fascicular areas and patterns [5, 6]. Alternatives such as allogeneic nerve transplants or synthetic, non-biological conduits exist [7, 8], but all options today have numerous shortcomings and outcomes are suboptimal [2]. Therefore, a reliable, high-quality, and widely available alternative is highly desirable in the repair of large-gap PNIs [2].

The goal of surgical repair with NCs is to facilitate a complex, natural repair process thereby maximizing the potential for the reinnervation of distal targets. Within 24 hours of nerve trauma, an irreversible cascade of apoptosis known as Wallerian degeneration occurs characterized by the dissolution of axonal cell membrane and cytoskeleton, release of axoplasm, retraction of the proximal and distal nerve stumps, and chromatolysis, the disruption of neurotransmitter production necessary for synaptic activity and axonal growth [9]. Schwann cells and macrophages phagocytose myelin and axon debris, and release neurotrophic growth factors, such as GDNF, NT-3, and NGF, creating a microenvironment favorable for axonal repair [10]. Despite degradative protease activity, basal laminae are spared leaving channels formed from residual endoneurial structures to direct an axonal growth cone emerging from Nodes of Ranvier at the proximal site towards a downstream synaptic target. Components of the conserved extracellular matrix (ECM), such as transmembrane cell adhesion molecules, laminin, fibronectin, and glycosaminoglycans (GAGs) provide stimulation of neuronal activity, Schwann cell migration [11], and modulation of neurite extensions resulting in regeneration at a rate of 1-2 mm/day [2, 12].

In the repair of large-gap PNIs, many conduits are unsuitable [2, 13, 14] due to mechanistic limitations. An unguided growth cone will result in a disorderly axonal mass forming a neuroma, a clinically painful outcome [15]. Optimal nerve conduits should contain a matrix-rich ECM scaffold, Schwann cells, neurotrophic growth factors, and a fascicular area comparable or greater than that of the injured native nerve. Material properties such as plasticity, durability, and tensile strength should be sufficient to resist mechanical injury [5, 10, 16]. In addition, research indicates that return of perfusion is critical, as diffusion of oxygen, nutrients, and cytokines relies on a network of longitudinally arranged blood vessels that courses throughout the nerve [17]. Therefore, vasculature that can be co-opted to restore perfusion would be advantageous [18]. Lastly, manufacturing ability, storage, and clinical acceptability are other critical considerations.

Viable xenogeneic nerve transplants offer the potential for a biological nerve conduit comprised of mixed-modal nerves which can facilitate nerve recovery in large-gap PNIs and also support efferent and afferent conduction through the conduit, without the additional morbidity and paresthesia from self-harvest and limitations of clinical availability.

Previously, the use of wild-type xenografts was explored, yielding mixed results. Evans et al. [19] reviewed all published research of xenograft nerve repair from 1880 to 1991, spanning more than 40 studies and hundreds of human and non-human subjects in which nerve sources were predominantly dog, rabbit, and rodents as nerve sources. However, general optimism for xenografts diminished after research and experience demonstrated inferior outcomes as compared to autografts [14, 20], as well as undesirable immunological responses [19, 21–23]. The adverse immunological responses are now understood, in the case of human recipients, to be primarily mediated by preformed antibodies against Galactose-α-1,3-galactose (α-Gal), an oligosaccharide expressed on all non-primate mammalian cells [24]. In some instances, xenografts were decellularized to diminish the rejection phenomenon as well as the possibility of zoonosis, but this resulted in the loss of essential cell populations in the process [2].

Surprisingly, few of these studies investigated the potential of porcine nerves given the greater physical and genetic similarities between *Sus Scrofa* and *Homo Sapiens*. Only recently has interest in the use of porcine donors gained momentum but limited research exists.The similarity of

critical physiological characteristics between pig and human nerves, including size, length, architecture, and extracellular matrix composition [1, 25–28], would suggest potential for regenerative capacity.

Advances in genetic engineering have permitted the creation of GalT-KO porcine donors that no longer expression the α-Gal-antigen, as well as mitigation strategies and treatments for zoonosis have since been developed [21, 24, 29–33]. Thus, we hypothesized that instead of traditional xenografts, viable xenogeneic nerve transplants derived from specialized, Designated Pathogen Free (DPF), GalT-KO porcine donors could offer an alternative solution for repair of large-gap (4 cm) PNIs.

Here, in a two-phase, 12-month pilot study, we report successful axonal regeneration, distal muscle reinnervation, and recovery of conduction velocity following surgical repair of fully transected radial nerves in 10 Rhesus Macaque recipients via the use of xenogeneic nerve transplants.

Results

Clinical Outcomes

All ten subjects tolerated the surgical procedure resulting in the complete loss of radial nerve function bilaterally (Figs. 1a, b, c). Nineteen of the 20 surgical transplant procedures were successful. In one subject, histomorphological analysis at necropsy revealed a large neuroma proximal to the transplantation site as well as the lack of axonal continuity through and distal to the transplant indicating failure to maintain coaptation at the proximal anastomotic site. Thus, all functional, electrophysiological, and morphological data for both of the transplant types from this subject were removed from nerve analyses, but clinical data were retained to assess immunological and toxicological outcomes.

Over the entire course of the study, no adverse events, negative veterinary observations, or other deleterious systemic effects attributable to the xenotransplant were observed in any subject. At necropsy, there were no abnormal findings during inspection of internal organs and other tissues in any recipient, regardless of tacrolimus regimen. Hematology and chemistry analysis were within normal ranges [34, 35]. Red blood cell (RBC), platelet (PLT) counts, hemoglobin (HGB), mean corpuscular volume (MCV), hematocrit (HCT), urea nitrogen (BUN), creatinine (CREA), and electrolyte levels were unremarkable for all subjects [36, 37].

In Phase 1, during which all ten subjects received 0.15 mg/kg/day of oral tacrolimus for the first six months of the study, no serious adverse side effects, such as diarrhea, cachexia, or other effects were observed in any of the ten subjects. Postoperative trough levels for the first six months were maintained below 35 ng/mL, and varied between individual recipients (4.9 to 32.2 ng/mL).

In Phase 2, during which five subjects continued the regimen (Group 1) and five subjects ceased tacrolimus treatment (Group 2), gradual weight increase was observed in Group 2 recipients, and all survived without incident to the 12-month end of study.

However, subjects in Group 1 presented with progressing symptoms associated with tacrolimus toxicity [38], such as limited mobility in knee joints, muscle rigidity, stiffness, and atrophy, as well as significant weight loss. As a result of the tacrolimus-associated toxicity, at 8-months, the five subjects in Group 1 were euthanized.

Functional Evaluation

During Phase 1, the rate of functional recovery qualitatively appeared to be slower in the xenotransplanted limbs (Figs. 1d, e, f). However, at the respective endpoints in Phase 2, there was no qualitative difference in the overall magnitude of functional recovery between limbs treated with a xenogeneic nerve transplant and the autologous control.

Electrophysiology

For all 18 limbs, preoperative median motor nerve conduction velocity was 64.26 m/s with an interquartile range (IQR) of 0.66 (Fig. 2a), and median sensory nerve conduction velocity was 53.72 m/s with an IQR of 0.11 (Fig. 2b). At the first postoperative assessment (5-months), there was an overall reduction in median nerve conduction velocities: motor, 36.50 with an IQR of 12.17 for autologous treated limbs; 50.33 m/s with an IQR of 21.16 for xenogeneic treated limbs, and sensory,

25.00 with an IQR of 13.50, autologous; 22.00 m/s with an IQR of 4.50, xenogeneic. In Phase 2, at 8-months postoperative, partial remyelination of fast-conducting fibers had occurred, indicated by an increase in median motor nerve conduction velocities:

56.33 m/s with an IQR of 13.01, autologous, and 57.00 m/s and an IQR of 11.83, xenogeneic (Fig. 3a). However, median sensory nerve conduction velocity did not return to preoperative baseline levels, only reaching 27.00 mV with an IQR of 12.5, autologous, and 27.00 mV with an IQR of 7.5, xenogeneic (Fig. 3b). At 12-months postoperative, the remaining four recipients in Group 2 demonstrated an increase in median motor nerve velocity of 62.17 m/s with an IQR of 8.76 and 63.34 m/s with an IQR of 4.33, autologous and xenogeneic treated limbs, respectively (Fig.

3a). Sensory nerve conduction velocity medians were statistically unchanged: 25.50 m/s with an IQR of 4.00, autologous treatment group and 27.5 with an IQR of 3.00, xenogeneic (Fig. 3b).

Median preoperative CMAP amplitudes for all 18 limbs was 20.03 mV with an IQR of 4.54. At 5-months, a nearly complete loss of action potential was observed in all limbs: 1.93 mV with an IQR of 1.41, autologous; 2.05 with an IQR of 2.08, xenogeneic), levels at which nerves would be unable to reach threshold firing levels (Fig. 2c). At 8-months, CMAP amplitudes for the autologous nerve transplants had recovered to 9.20 mV with an IQR of 4.27, compared to a CMAP of 7.30 mV and an IQR of 6.13, xenogeneic (Fig. 3c). However, at 12-months, there was a significant increase in CMAP amplitude magnitudes for both types of transplants with a median of 15.44 mV and IQR of 4.64 for autologous and 14.15 with an IQR of 4.83 for xenogeneic.

Preoperative CMAP duration median values for all 18 limbs were 3.98 ms with an IQR of 0.12 (Fig. 2d). At 5-months, durations changed to 3.14 ms with an IQR of 3.27 for autologous treatment sites and 5.12 ms with an IQR of 2.66 for xenogeneic treatment sites. Over the course of the study, however, there were no statistical differences in CMAP durations between the limbs treated with either transplant type, with maximum recovery observed at 8-months postoperative (4.81 ms with an IQR of 1.71 ms, autologous; 4.62 ms with an IQR of 1.99 ms, xenogeneic) (Fig. 3d).

Overall, by the respective Phase 2 endpoints, there were no statistically significant or physiologically relevant group differences in motor or sensory conduction velocities, CMAP amplitude or duration between the autologous or xenogeneic reconstructed limbs. All statistical analyses performed using Student's t-test; ns = not significant with a $P \leq 0.05$.

Immunogenicity

Across both Phase 1 and Phase 2, white blood cell count (WBC) and individual component percentages remained within normal ranges [36, 37] (Fig. 4a, b). Neutrophil and lymphocyte percentages varied month-to-month, but absolute counts remained close to expected values (2.40 ± 6.18 K/μL and 2.46 ± 8.94 K/μL respectively).

Total IgM levels were slightly elevated above preoperative levels at one or more postoperative time points in all recipients (Fig. 4c). The highest level of total IgM and IgG were observed 1-month postoperative. Overall, changes detected in total serum IgM and IgG levels did not vary more than 50% from baseline levels for each individual recipient in Groups 1 and 2 and remained stable over the course of the 12-month study.

Anti-porcine IgM and IgG levels showed an increase above preoperative levels following transplantation followed by a gradual decrease to baseline values over time (Fig 4d). The highest IgM fold increases were detected for all recipients at one week (0.25 months) and 3-months, and the highest IgG fold increases were detected for all recipients in 1 and 3-months.

Histology

Blinded histological analysis found no meaningful differences between nerve tissue excised from transplantation sites in limbs treated with either autologous or xenogeneic transplants.

Nerve bundle diameter for perioperative explanted nerves not used for transplantation were >300 μm. For Group 1, the diameter of the regenerated nerve bundles across the defect site for all five recipients was comparable for both types of nerve transplants, ranging from 100 to 300 μm. At the end of study for Group 2, xenogeneic nerve bundle diameters appeared smaller than those of th autologous control, with four autologous controls reaching preoperative diameters (Figs. 5a, b).

Overall, for all recipients and transplant types, full myelination in the nerve regions immediately proximal to the transplanted sites was observed, with discernible loss of myelin in regions distal to the transplants. For xenogeneic transplants, little to no myelination was observed in subjects from either group. Overall, autologous transplants appeared to result in regenerated nerves with a greater presence of myelination. (Figs. 5c, d).

The degree of cell death (necrosis) and presence of fibrotic tissue (fibrosis) were comparable between tissue from autologous and xenogeneic transplant sites (Figs. 5e, f). Enlargement of the nerves was observed at the proximal and distal anastomotic sites for both types of transplants in all recipients (Figs. 6a, b). In the transplanted regions, there was mild fibrosis with embedded nerve fibers coursing mostly longitudinally along the long axis of the transplant. The extent of the fibrous tissue present was consistent with the damage incurred as a result of the surgical procedure. Microscopic examination demonstrated foreign body reaction around the sutures, as well as multidirectional proliferation of small diameter nerve branches causing minor neuroma formation on all transplants, smaller in scale than that of the one surgical transplant failure.

There was a notable difference in the infiltration of inflammatory cells at the transplant sites between xeno-and-allo reconstructed limbs. At 8-months, the overall inflammation for the autologous treated limbs was observed to be minimal with scattered lymphocytes and macrophages (Fig. 6c). In contrast, the xenogeneic transplantation sites had a greater degree of inflammation consisting of lymphocytes and macrophages

(Fig. 6d). Similarly, by the 12-month time point the xenogeneic treatment group showed more lymphocytes, macrophages, and inflammation than the autologous treatment group. Also, there were distinct tertiary lymphoid follicles scattered throughout the nerve sample (Figs. 6e, f).

Biodistribution of Porcine Tissue

Chimerism and PERV copy number and expression were analyzed to assess the presence of porcine cells by both conventional and Q-PCR. Samples analyzed included xenogeneic and autologous nerve tissues harvested at 8- and 12-months postoperative, sera and PBMCs from the ten subjects obtained at various timepoints over the 12-month study, and spleen, kidney, liver, heart, and lung samples obtained at necropsy. Recipient PBMCs, sera, and tissues tested negative for PERV RNA and/or DNA amplification or microchimerism, indicating that there was no evidence of microchimerism or circulating porcine cells in any of the tissues/cells analyzed. Sera was also found negative for PERV RNA expression indicating that no active replication appeared to be taking place. All samples were positive for either the internal positive control (sera) or the control 18s housekeeping gene indicating the validity of the analysis (Table 1).

The autologous nerve grafts lacked the presence of PERV or porcine cells. Surprisingly, the xenogeneic sites were also negative for the presence of porcine cells by Q-PCR suggesting there was no residual porcine tissue in the xenogeneic nerve tissue tested. Q-PCR for the porcine centromere was also negative (Table 1). However, the use of a primate specific primer set using conventional PCR demonstrated the presence of primate cells in both autologous and xenogeneic transplants (Fig. 6g).

Discussion

Physical guidance and Schwann cell activity are vital components of nerve repair, and optimal axonal regeneration depends on growth in a conducive and complex biological environment. Thus, the therapeutic capacity of any nerve conduit, especially one sourced from a foreign species, is correlated to its ability to mirror the conditions of the host environment.

Porcine nerves are well suited for this task, as many essential properties are conserved, closely resembling the neuroanatomy of humans. Characterization studies reveal length, number, pattern, and fascicular area to be comparable [1, 17, 27, 39–42]. This is highly favorable as endoneurial alignment and matched fascicular cross-sectional areas improve clinical outcomes. The architecture, composition, and distribution of essential components of the porcine ECM, such as collagen, laminin, fibronectin, and GAGs such as hyaluronic acid and chondroitin-4-sulfate are also highly similar [20, 43], resulting in clinically advantageous structural integrity, Young's modulus, and tensile strengths [17, 27]. These characteristics allow for enhanced reliability of sutures to maintain stable coaptation under tension. Location and quantities of Schwann cells distributed throughout the perineurium and endoneurium of porcine peripheral nerves closely mirror that of human nerves [44].

It could be inferred that these features are responsible for the neuroregenerative capacity of the xenogeneic nerve transplants used in this study. The regrown peripheral Rhesus Macaque nerve was capable of reinnervation of the extensor digitalis, allowing functional recovery and statistically equivalent electrophysiological and morphological outcomes to the autologous control. This is noteworthy given the comparator's known advantages: the injury was repaired with a graft of the same type, size, and immediately after axonotomesis. These are ideal conditions, unrealistic in a clinical setting. Instead, direct comparison against other nerve conduits would be a more clinically relevant.

Recovery of compound muscle action potentials and conduction velocities indicate adequately myelinated, fast-conducting fibers were restored, suggesting a successful mixed-modal repair which would be expected to improve over time [2]. The xenogeneic transplant was able to sufficiently replicate the conditions necessary to support fundamental repair mechanisms, despite its foreign origin [20, 43, 45, 46]. Further, these outcomes were successful in large-gap PNI, where as nerve conduits are often limited to shorter defects. Clinical studies have shown Avance® to support nerve regeneration of limited distances, and the number of new fibers was only 30% of those achieved using autologous nerves [46–48].

Given that the loss or absence of Schwann cells diminishes regenerative capacity and leads to poor outcomes [46, 49–51], these results suggest the xenotransplants provided sufficient quantities of Schwann cells able to adequately function despite their exogenous source. This finding warrants further evaluation but is plausible as the interchangeable use of cross-species cells, tissues, and organs have been previously demonstrated [1, 27, 52–59].

The greatest difference between the two transplants was the presence of tertiary lymphoid nodules located on the regenerated nerves in xenogeneic-treated limbs. These follicles, comprised of macrophages and dendritic cells, are likely a result of a localized immune response to the porcine material, despite lacking the α-Gal-moiety, further indicated by the post-operative presence of anti-porcine antibodies. The magnitude of the immune response, however, was subdued enough as to not result in symptoms or signs related to graft rejection, which may be attributed in part to the concomitant use of tacrolimus. Tacrolimus is the most widely used immunosuppressive in nerve allotransplantation [2, 23, 60], and is also reported to accelerate the rate of nerve regeneration [2, 34, 60–68]. Thus, all subjects in Phase 1 received a clinically relevant dosage of oral tacrolimus for six months [38].

At 6-months, tacrolimus treatment was discontinued as an immunosuppressive for 5 subjects but was continued for the subjects in Group 1 to assess whether prolonged use conferred any further neuroregenerative benefits. As demonstrated by the toxicity exhibited at 8-months, the prolonged use of tacrolimus was not justified and may actually have impeded Schwann cell migration [69]. Further, future studies may demonstrate that tacrolimus is unnecessary for nerves from GalT-KO porcine donors. If meaningful therapeutic benefit can be afforded by a single knockout without the need for immunosuppression, this would suggest that a larger platform of temporary, but clinically useful, viable xenotransplants may exist.

At the rate of 1 mm/day, the cellular components of the 4-cm porcine transplant were expected to be fully replaced and repopulated by the host cells [19, 62, 69], culminating in the complete, macrophage-mediated clearance of porcine cellular material and elimination of immunogenic porcine antigens. This was supported by the lack of detectable porcine DNA or RNA using Q-PCR in both the xenogeneic and autologous nerve tissue at necropsy. In addition, assessment of blood and tissue from the recipients indicated no circulating porcine cells or replication of PERV elements. Both housekeeping Q-PCR and qualitative PCR assays detected DNA in the nerve samples, however, initially it was not possible to differentiate between primate and porcine as the control assays were not specific. Conventional PCR utilising a primate specific gene did indeed show that primate cells were detectable in both the autologous and xenogeneic transplants.

Previous testing of skin xenotransplants had demonstrated that porcine cells were detectable at the graft site but as found here, this did not extend to the peripheral circulation [70], which did not appear to be the case for this study. Given the lack of detection here and the immunological responses shown, this supports the expectation that the porcine transplant is fully replaced and repopulated by the host cells. These methods are highly sensitive and specific and are of more value than, for example, immunohistochemistry, which in addition to lack of sensitivity, can be complicated by the lack of suitable antibodies to distinguish cell content. Indeed, recently, it has been suggested that the use of PERV genes for detection increases the sensitivity of the molecular assay and may also be indicative of an inflammatory reaction in addition to testing for infection as is done for allo-transplants [71]. No significant reaction was seen in these animals again reflected in the lack of detection. Whilst Rhesus Macaques are currently not considered a suitable model for PERV infection [72], this limitation does not affect this study as our intention is to assess the presence or absence of porcine cells using the best tools possible.

Aspects of the study design, such as the use of Rhesus Macaques, selection of the radial nerve, dosing regimen of tacrolimus, and cryopreservation were chosen to provide clinically relevant data while balancing the ethical use of animal subjects. The use of one porcine donor controlled for variation in morphology and physiology of the nerve transplant in this study, which would be expected to be consistent if sourced from a genetically- and age-matched animal from the same closed colony. Cryopreservation is a well characterized process that preserves cell viability, basal lamina, and endoneurial structure [11, 14, 63], as well as, in this case, limited variability of surgical personnel, techniques, and conditions. There were no significant differences in outcome measures between fresh and frozen transplants. The subjectiveness intrinsic to qualitative analyses was mitigated by the use of relative parametric comparisons by experienced professionals blinded to the nature of the test article.

Combined, our long-term, in vivo data presented herein suggests promise for the repair of large-gap PNIs via the use of viable, GalT-KO porcine nerve transplants. These data also highlight the potential for inter-species cellular compatibility which could have positive implications for future cell therapies. Further evaluation is required, but these results are encouraging for neural porcine therapies and more broadly support the clinical potential of the field of xenotransplantation.

Methods

Animals

This study's surgical procedures, protocols, and guidelines for animal care were independently IACUC reviewed and monitored to ensure the ethical treatment of animals. The Test Facility is accredited by the Association for the Assessment and Accreditation of Laboratory Animal Care, International (AAALAC) and registered with the United States Department of Agriculture (USDA) to conduct research in laboratory animals. The veterinary care of the animals were in accordance with the protocol, Test Facility's SOPs, and regulations outlined in the applicable sections of the Final Rules of the Animal Welfare Act regulations (9 CFR Parts 1, 2, and 3), the Public Health Service Policy on Humane Care and Use of Laboratory Animals, the Guide for the Care and Use of Laboratory Animals, the U.S. Food and Drug Administration (FDA) Good Laboratory Practice (GLP) regulations, standards, and guidelines (US-FDA 21 CFR Part 58.351 and GFI 197), in accordance with ARRIVE guidelines, and the Biomere, Policy on Humane Care. The protocol and any amendments or procedures which involved the care or use of animals in this study were reviewed and approved by the Test Facility's Institutional Animal Care and Use Committee (IACUC) before the initiation of such procedures.

All xenogeneic nerve transplants used in this study were sourced from one genetically engineered α-1,3-galactosyltransferase knock-out (GalT-KO), designated pathogen free (DPF) porcine donor [70]. Five male and five female na¨ıve Rhesus Macaques (Macaca mulatta) served as xenogeneic nerve transplant recipients.

Cryopreservation

Samples were packaged in cryovials (Simport, T310-1A, Beloeil, QC). Cryoprotective media (5 mL, CryoStor CS5 media, BioLife Solutions, Bothwell, WA) was added to each vial before it was sealed and cryopreserved using a controlled rate freezer at 1°C per minute. The frozen cryopreserved nerve xenotransplants were stored at -80°C, and the ones stored in media were maintained at 4°C until use (24-48 hours).

Surgical Procedures

The porcine donor was euthanized and prepared for surgery as previously described [70]. To isolate the sciatic nerve prior to harvesting, a linear incision was made midway between the sacrum and the ischium and extended ventrally along the posterior aspect of the femur, longitudinally dissecting the gluteus medius, gluteus maximus, piriformis, and biceps femoris muscles, to the proximal tibiofibular joint (Fig. 1a, b). The sciatic nerve was visualized and harvested by radial transections distal to the nerve origin and proximal to the bifurcation into the tibial and common peroneal nerves. This process was repeated on the bilateral side.

One unmodified sciatic nerve segment was stored in RPMI media and maintained at 4°C until surgical use 48 hours later, which was segmented into five xenogeniec nerve transplants, used as the source of the donor nerve to repair the radial nerve defect in 5 Rhesus Macaque recipients. The bilateral porcine sciatic nerve was cryopreserved per protocol, and stored at -80°C for a period of 7 days, after which it was thawed per protocol [52], and used as the source of the donor nerve to repair the radial nerve defects in the remaining 5 Rhesus Macaque recipients. Cryopreservation of the sciatic nerve was necessary to limit variability of surgical personnel, techniques, and conditions, as the number of surgeries and availability of surgical team required more than one series of surgical operations. Preservation of the nerve material at 4°C for this extended timeframe was deemed likely to impair the quality of the nerve material, whereas cryopreservation is a well characterized process that preserves cell viability, basal laminae, and endoneurial structure [11, 14, 63].

Prior to transplantation, xenogeneic nerves were trimmed to 4 cm to fit the defect size. Large-gap (4 cm) peripheral nerve defects were surgically introduced bilaterally in all ten Rhesus Macaque recipients. Recipients, under anesthesia [73], were positioned in lateral recumbency with the shoulder at 90º flexion, full internal rotation, and neutral abduction. The subcutaneous tissue and deep fascia were dissected for anatomical orientation. A 6-8 cm skin incision was made along the posterolateral margin of the proximal arm towards the antecubital fossa. This procedure exposed the long and lateral heads of the triceps, which converge to form the triceps aponeurosis [74]. The intramuscular plane between the long and lateral head of the triceps was developed approximately 2.5 cm proximal to the apex of the aponeurosis where the radial nerve and accompanying vessels were observed against the humerus in the radial groove. The surgical plane was extended proximally and distally to minimize unintended injury. The radial nerve was distally transected approximately 1 cm proximal to the origin of the deep branch. A 4 cm segment was removed to create the defect and saved for reattachment or subsequent analysis.

Nerve transplants were attached proximally and distally with four to eight equidistant 8-0 nylon monofilament sutures at each neurorrhaphy site. The incision was then closed in layers using subcuticular, absorbable sutures. This process was performed bilaterally per each of the ten recipients; both xenogeneic and autologous nerves were transplanted in the same surgical procedure. Limb designation (right/left) for xenogeneic or autologous transplants was randomly assigned and blinded from observers for analysis. The ten recipients were randomly, evenly divided between two surgical series, one week apart. Five fresh xenogeneic transplants were used in the first series, and five thawed, previously frozen viable porcine xenogeneic transplants were used in the second.

Porcine sciatic nerve was selected as the source of the xenogeneic transplant due to its superstructural similarity to human and primate nerve [1]. The radial nerve was selected as the transplantation recipient site because there are minimal neighboring nerves. Those in close proximity may reinnervate downstream muscle fibers and complicate electrophysiology and functional analysis of the extensor digitalis muscles. Transplantation at the radial nerve also allowed for ethical loss of function and clearly articulated return of function in an observable and isolated movement. The maximum practical gap size possible was 4 cm based on the measured lengths of the recipients' limbs. The mean distance from the recipients' proximal neurorrhaphy site to the site of innervation of the extensor carpi radialis longus and extensor carpi radialis brevis muscles [35] measured 15.7 ± 0.17 cm. Bilateral, 4 cm complete transections of radial nerves were surgically introduced in a total of ten Rhesus Macaque recipients. Two porcine sciatic nerves were harvested from one donor (Fig. 1a), trimmed into ten 4 cm segments (Fig. 1b) and transplanted into one of the radial nerve gaps in each recipient (Fig. 1a), randomized to the left or right limb. In the contralateral arm, excised Rhesus Macaque radial nerve segments were rotated 180°and reimplanted as a surgical control (Fig. 1a). Surgeries were performed synchronously, and the surgical personnel, sterile field, surgical technique, and uniformity of the transplant procedure were independently assessed for quality control at each step.

Due to the large number of surgeries, five sciatic nerve segments were transplanted fresh one to two days after donor harvesting while the remaining five were cryopreserved and subsequently thawed for transplantation over two days the week following based on Holzer et. al., 2020 [70]. Cryopreservation of xenogeneic skin transplants has been shown to be safe and effective for up to seven years [75], demonstrating no significant or meaningful differences between fresh and frozen transplants.

Upon recovery, nerve tissues were immersed in antibiotic solution for decontamination and underwent longitudinal microbiological testing during processing: if a microbiological culture yielded microbial growth, the tissue was discarded. Before the freezing, tissues were immersed in a storage solution composed of RPMI1640 with L-glutamine (Sigma-Aldrich) containing 5% dimethyl sulfoxide as cryoprotectant (Bio-Life Solutions CRYOSTOR-5). Each tissue was preserved in cryoprotective vial and placed in a liquid nitrogen computer-controlled freezer that facilitates a controlled decrease in temperature (1°C/minute) to –80°C. After the freezing, the tissues were stored at –80°C until being thawed in a 37C water bath prior to use.

Toxicology

Oral administration of tacrolimus, at a dosage of 0.15 mg/kg/day, began 14 days before surgery and was continued until 6-months for subjects in Group 2, and 8-months for Group 1.

Pathology

At the designated necropsy time point, the animals will be sedated with Ketamine (10 - 15 mg/kg, IM). An IV catheter will be placed and euthanasia will be performed by administration of Euthasol (≥ 50 mg/kg or to effect, IV). Explants of the entire autologous or xenogeneic transplant, including proximal and distal nerve, as well as samples of spleen, liver, kidney, lung, and heart were collected, fixed in 10% neutral buffered formalin, and transferred to 70% ethanol after approximately 72 hours. Nerve explants were trimmed longitudinally, routinely processed and embedded in paraffin blocks. Resulting blocks were sectioned and stained with either hematoxylin and eosin (H&E), Luxol Fast Blue (LFB), or immunohistochemically stained for neurofilament H (NF-H). Spleen, liver, kidney and heart were trimmed, processed, embedded in paraffin, sectioned and stained with H&E. All tissues were evaluated in a manner blinded to treatment. Nerve explants were evaluated for morphologic changes and underwent semi-quantitative scoring according to the criteria in Table 1. All measurements of axon diameter were made by the pathologist using an ocular micrometer.

At necropsy samples of the spleen, liver, kidney, and other organs were collected. PERV copy number and expression were analyzed by Q-PCR to assess the presence of PERV DNA and mixed chimerism. Samples analyzed included xenogeneic and autologous nerve tissues harvested at 8- and 12-months postoperative, sera and PBMCs from the nine subjects obtained at various time points over the 12-month study, and spleen, kidney, liver, heart, and lung samples obtained at necropsy.

Biodistribution

To confirm whether porcine or primate tissue was present, qualitative PCR using a primate specific target gene demonstrated the presence of primate cells in both autologous and xenogeneic transplants (Fig. 6a). All samples were positive for either the internal positive control (sera) or the control reference genes indicating the validity of the analysis (data not shown).

Histopathology

Explanted tissues were stained by immunohistochemistry for expression of Neurofilament H to demonstrate axons (Fig. 5a). Luxol Fast Blue staining was used to demonstrate myelination levels of the various regions of the explant (Fig. 5c).

Electrophysiology

Sensory and motor nerve conduction was evaluated for all nine recipients in both arms at baseline and postoperatively at 5-, 8-, and 12-months [76] using Natus UltraPro with Electrodiagnostic software [35]. Motor nerve function was assessed across the length of the radial nerve by eliciting orthodromic compound muscle action potentials from the extensor digitorum communis muscle (EDC) via stimulation at four locations proximal and distal to the transplant site. Motor conduction velocity (NCV), compound muscle action potential (CMAP) amplitude and CMAP duration were calculated for each location following the last supramaximal stimulation and then averaged across the nerve sites. Sensory nerve conduction was determined by eliciting sensory antidromic nerve action potentials (SNAPs) directly from the distal branches of the radial nerve as it passes over the extensor pollicis longus tendon. Approximately ten supramaximal stimuli were averaged for each sensory nerve conduction velocity calculation.

Evaluations [76] and analysis were performed using a Natus Neurology System. All motor and sensory responses were elicited with a pediatric stimulator and subcutaneous needle electrodes were used for recordings. Recording procedures were adapted from routinely used neurological clinical protocols. Motor nerve recordings were performed orthodromically at the extensor digitorum communis (EDC) muscle, with successive

orthodromic stimulations in the antecubital fossa, at the spiral groove, across the transplant, and at the axilla between the coracobrachialis and the long head of the biceps. Sensory nerve action potentials were recorded antidromically from the radial sensory branch over the extensor pollicis longus tendon with stimulation over the radial side of the forearm, 5 cm proximal. The motor NCV for each segment was calculated using the differences in onset latency and distance between each two points of stimulation along the radial nerve following supramaximal stimulation. Values were averaged to provide an overall mean of each recipient's motor NCV per arm. CMAP amplitude was determined at the peak of the response following supramaximal stimulation of the associated nerve and the CMAP duration marked at the repolarization. Segmental conduction velocities across the radial nerve were averaged. Sensory nerve responses from approximately ten supramaximal stimuli were averaged at each time point. The conduction velocity was calculated using the onset latency of the response and the distance (for sensory NCV) or the distance difference (for motor NCV) from the stimulation cathode to the recording site.

Functional Evaluation

A previously reported radial nerve injury mode [77] was adapted to assess the functional recovery of xenogeneic and autologous nerve transplant recipients. Radial nerve injury proximal to the elbow results in a loss of wrist extension function, or "wrist drop," loss of forearm muscle tonality, and digital extension due to motor denervation of the extensor carpi radialis longus and extensor carpi radialis brevis muscles [78, 79]. Radial nerve functional assessments were performed monthly for each recipient and included chair and cage-side observations of active and passive wrist angle flexion during the recipient's retrieval of objects requiring wrist angle extension to obtain them. A series of wrist extension and gripping attempts by each recipient were video recorded, for each isolated arm, for each month. Observations were performed using food treats or mechanical stimulation to encourage wrist extension and gripping. This resulted in 16:13:33 hours of data, for 18 limbs of nine Rhesus Macaque transplant recipients. Over the entire study period a combined 2,057 total events were recorded. Results were analyzed by two independent investigators in a blinded manner with respect to the transplant type and location.

Qualitative regain of radial nerve functionality was monitored according to the following categorical scale: no observable impairment (Fig. 1d), mild impairment, moderate impairment, and severe impairment (Fig. 1e).

Immunogenicity

Total serum IgM and IgG (Fig. 4d) were measured using a commercial ELISA and overall median and IQR were found all nine animals included in the study. Binding of xenoreactive antibody to pig cells was measured as previously described [80]. Cryopreserved genetically modified α-1,3-galactosyltransferase knockout (GalT-KO) porcine PBMCs were thawed, and cell concentration was determined using Coulter MD II (Coulter Corporation, Miami, FL). Cells were diluted to a concentration of 1.5 x 106 cells/mL in FACS buffer (1X Hanks' Balanced Salt Solution (HBSS) with calcium and magnesium, 0.1% BSA, and 0.1% sodium azide). Decomplementation of the serum samples was carried out by heat inactivation for 30 min at 56 ºC and diluted at 1:2, 10, 100, 1,000, and 10,000 ratios using FACS buffer. 100 µL of the cells were added into each well in 96-well u-bottom plate with 10 µL of the diluted serum samples and incubated for 30 min at 4 ºC. Cells were washed one time using 200 µL FACS buffer. To prevent nonspecific binding, cells were incubated in 100 µL 10% goat serum for 10 min at room temperature followed by one more additional washing. Cells were stained with goat anti-human IgG PE and goat anti-human IgM FITC (Jackson ImmunoResearch Laboratories Inc., West Grove, PA) for 30 min at 4 ºC. Cells were washed two times using FACS buffer and resuspended in 200 µL 0.5% PFA in MACS/1X PBS buffer. Flow cytometric analysis completed on Novocyte flow cytometer (ACEA Biosciences, Inc. San Diego, CA). Flow cytometry data was analyzed using NovoExpress 1.3.0 (ACEA Biosciences, Inc.).

Binding of IgM and IgG was assessed using relative mean fluorescence intensity (MFI): Relative Actual MFI value/MFI obtained using secondary antibody in the absence of serum. IgG and IgM ELISA kits from Life Diagnostics were used for the quantification of total circulating IgG and IgM in Rhesus serum by following the manufacturer's instructions.

Recipients were iteratively assessed for anti-porcine IgM and IgG antibodies to evaluate their response to peripheral blood mononuclear cells (PBMCs) from GalT-KO porcine donors, and for total circulating IgM and IgG levels to assess changes in systemic immunogenicity over the course of the study (Figs. 4c, d). These are measurements of circulating IgM and IgG levels in each recipient, therefore each data point in Figures 5a-d represents one recipient Rhesus Macaque, not the xenogeneic or autologous limb. Importantly, tacrolimus withdrawal at 6-months did not increase Group 2 total or anti-porcine IgM or IgG.

Binding of anti-porcine IgM and IgG was assessed using Median Fluorescence Intensity (MFI) and relative MFI obtained as follows: Relative MFI = Actual MFI value / Limit of Blank (MFI obtained using secondary antibody only in the absence of serum).

PCR

Twenty milligrams of the xenogeneic porcine tissue samples and 7 mg of autologous primate tissue samples were treated with the DNeasy Blood and Tissue Kit (Qiagen, Crawley, UK) as described by the manufacturer that included the RNase A-treatment step. The isolated DNA was quantified by UV spectrophotometry. Quantitative PCR amplification of 18S (Eurogentec, Seraing, Belgium) was carried out to assess the DNA homogeneity across samples. Serum samples were processed using the Viral RNA mini kit (Qiagen, Crawley, UK) as described by the manufacturer incorporating the DNA digestion step using DNase I to isolate viral RNA. Samples were then processed using the RNeasy MinElute Cleanup kit (Qiagen, Crawley, UK). All Serum samples shown to have an IPC CT <32 progressed to PERV transcription analysis. PMBC samples were processed for DNA isolation using a modified version of the manufacturers “Whole Blood” protocol for the Gentra Puregene Blood kit (Qiagen, Crawley, UK). The modified protocol involved homogenizing the PBMC samples prior to RNase A treatment, protein precipitation and finally isopropanol and 70% ethanol washes were added before DNA hydration. The DNA product was quantified using UV spectrophotometry and 18S amplification carried out to assess DNA homogeneity between samples while using 200 ng/reaction. PBMC samples shown to have an 18S CT <27 progressed to PERV copy number and mixed chimerism analysis. At necropsy, tissue samples of Kidney, Liver, Lung and Spleen were harvested. RNA isolation was conducted on 35 mg of the tissue samples using the RNeasy mini kit (Qiagen, Crawley, UK) with homogenization using a Fast-Prep 24 (MP Biomedicals, Eschwege, Germany). The RNA product was quantified using UV spectrophotometry and 18S amplification carried out to assess DNA homogeneity between samples while using 200 ng/reaction. Tissue samples shown to have an 18S CT <13 progressed to amplification, reverse transcription, and PERV copy number and mixed chimerism analysis.

Amplification was carried out using an Applied Biosystems ViiA 7 Real-Time PCR System with a polymerase activation step (10 min at 95 °C) and 40 amplification cycles of 15 sec at 95 °C, 30 sec at 53 °C, and 30 sec at 60 °C. All primate and porcine transplantation site samples shown to have an 18S CT <29 progressed to PERV copy number and mixed chimerism analysis. PERV genome copy number quantification and mixed chimerism was assessed by quantitative PCR (Q-PCR) using the QuantiTect virus kit (Qiagen, Crawley, UK), with identical cycling conditions described above. PERV was assessed using TaqMan primers specific to the PERV-pol gene as previously described [81]. PERV quantification was carried out by comparison to standards of known PERV copy number. The limit of quantification (LOQ) for PERV using this assay is ten copies per reaction. Mixed chimerism was assessed using TaqMan primers for porcine centromeric DNA that were also used in the study described [81]. Detection of porcine cells was quantified by comparison to standards of known porcine cell content. The LOQ for porcine cells using this assay is 0.026 cells per reaction.

Qualitative PCR for the reference gene RPL13A (ribosomal protein gene) was carried out to confirm DNA was suitable for amplification. Primers used were 5'-CCT GGA GGA GAA GAG GAA AGA GA-3' and 5'-TTG AGG ACC TCT GTG TAT TTG TCA AG-3' giving an amplicon of 126 bp. Fifty nanograms of DNA and 0.5 µM primers in a total volume of 25 µl was cycled under the following conditions; 5 min at 94 °C, 50x (10 sec at 94 °C; 15 sec at 58 °C; 15 sec at 72 °C) 10 min at 72 °C. This PCR will detect both primate and porcine material.

Detection of primate specific DNA was carried out using qualitative PCR as described previously [82] with modifications. In brief, primers used were P5 5′-ATC TGG ACC AGA AAT CCC GAC GAT ATT ACT AAT GAG GAG-3′ and P6 5′-CTT GTA GTT CTC TTT ATC TTC CGC CAG TTC AGT AAA GAG-3′ giving an amplicon of 450 bp. Using the Taq PCR core kit (Qiagen, Surrey, UK) 75 ng of DNA and 0.2 µM primers in a total volume of 50 µl was cycled under the following conditions; 94 °C for 5 min, 40x(30 sec at 94 °C, 30 sec at 5 °C, and 60 sec at 72 °C), 10 min at 72 °C. PCR analysis was preferred for specificity which is not seen by the use of antibodies to nerve components.

Hematology and Clinical Chemistry

Tacrolimus administration was initiated 5-14 days before surgical procedures via intramuscular injection in the ten Rhesus monkey recipients. Postoperatively, all recipients received tacrolimus for at least six months [76] and trough levels were maintained below 30 ng/mL.

Serum chemistry blood samples were processed for serum or transferred to the Biomere Testing Facility laboratory and processed. Whole blood hematology samples were transferred to the Testing Facility laboratory without processing. Whole blood was analyzed on an IDEXX Procyte analyzer for erythrocyte count, hemoglobin, hematocrit, platelet count, leukocyte count, reticulocyte count, and mean corpuscular volume, hemoglobin and hemoglobin concentration, Serum samples were analyzed using an IDEXX Catalyst analyzer (Chem15, Lyte4, Trig, and AST slides for A/G ratio, alanine aminotransferase, albumin, alkaline phosphatase, aspartate aminotransferase, calcium, chloride, cholesterol, creatinine, gamma glutamyl transferase, globulin (by calculation), glucose, inorganic phosphate, potassium, sodium, total bilirubin, total protein, triglycerides, and urea nitrogen.

Statistical Analysis

Data comparisons between autologous and xenogeneic nerve transplant sites, unless otherwise stated, are expressed as medians with interquartile ranges per transplant type. Statistical comparisons were performed as one-way analysis of variance tests with the Student-Newman-Keuls multiple comparisons method. Immunoglobulin analysis was performed as an unpaired t-test using Prism Graph Pad version 9.1.0 software (Prism, San Diego, CA USA). P values less than 0.05 were considered statistically significant for all analysis.

Declarations

Acknowledgements

The research reported in this publication was supported in part by the Department of Defense under Award Number W18XWH-17-I-0454. We thank Dana Barberio of Edge Bioscience Communications for her writing and editorial assistance on a previous version of this manuscript. We thank the animal care staff at Biomere for their assistance with this GLP study. The schematic figures were created with BioRender.com.

Author Contributions

P.H., C.L.C., and R.M. obtained the funding and designed the experiments. P.H. and

C.L.C. performed all animal surgeries. A.L. provided the animal facilities, resources, veterinary observations, and performed behavioral experiments, hematology, and clinical chemistry. M.M. performed electrophysiology. L.S., J.T., and N.G. performed PERV analysis and all PCR. J.W. performed all pathology. B.O. and A.L. performed immunogenicity assays. P.H., E.J.C., D.L., M.M., J.W., B.O., L.S., and R.M. performed data analysis. D.L. and E.J.C. drafted the manuscript. S.G., J.D., and all authors revised the manuscript for critical content. P.H., K.R., and J.A. managed all administrative, technical, or supervisory tasks.

Competing Interests

C.L.C. previously served as a board member of XenoTherapeutics, Inc, 501(c)3. L.S. is a member of the safety review board of XenoTherapeutics, Inc, 501(c)3. P.H., J.A., and C.L.C. are cofounders of XenoTherapeutics, Inc, 501(c)3. P.H., J.A., K.R., E.J.C., and R.M. are inventors on patent applications related to this work. P.H., E.J.C., D.L., K.R., J.A., and R.M., received financial compensation as employees of XenoTherapeutics, Inc, 501(c)3. Biomere, StageBio, and XenoDiagnositcs are paid vendors for XenoTherapeutics, Inc, 501(c)3. The other authors declare no competing interests.

Materials and Correspondence

The datasets generated during the current study are not publicly available due proprietary reasons but are available from the corresponding author, P.H., on reasonable request.

References

1. Zilic, L. *et al.* An anatomical study of porcine peripheral nerve and its potential use in nerve tissue engineering. *J Anat* **227,** 302–314. ISSN: 0021-8782. https: //www.ncbi.nlm.nih.gov/pmc/articles/PMC4560565/ (2019) (Sept. 2015).
2. Grinsell, D. & Keating, C. P. Peripheral nerve reconstruction after injury: a review of clinical and experimental therapies. *Biomed Res Int* **2014,** 698256. ISSN: 2314- 6141 (2014).
3. Johnson, E. O. & Soucacos, P. N. Nerve repair: Experimental and clinical evaluation of biodegradable artificial nerve guides. *Injury* **39,** 30–36. ISSN: 00201383. https : / / linkinghub. elsevier. com / retrieve / pii / S002013830800257X (2021) (Sept. 2008).
4. Li, R. *et al.* Peripheral Nerve Injuries Treatment: a Systematic Review. *Cell Biochem Biophys* **68,** 449–454. ISSN: 1085-9195, 1559-0283. http://link.springer.com/10.1007/s12013-013-9742-1 (2021) (Apr. 2014).
5. Vasileiadis, A. Bridging of Peripheral Nerve Defects by Autologous Nerve Grafting Personal Experience. *MOJ Orthop Rheumatol* **5.** Publisher: MedCrave Publishing. ISSN: 2374-6939. https:// medcraveonline. com/ MOJOR/ MOJOR- 05 - 00183 . pdf (2021) (Aug. 9, 2016).
6. Lee, S. K. & Wolfe, S. W. Peripheral Nerve Injury and Repair. *JAAOS - Journal of the American Academy of Orthopaedic Surgeons* **8,** 243–252. ISSN: 1067-151X. https://journals.lww.com/jaaos/Fulltext/2000/07000/Peripheral Nerve Injury and Repair.5.aspx (2021) (Aug. 2000).
7. Griffin, J. W., Hogan, M. V., Chhabra, A. B. & Deal, D. N. Peripheral Nerve Repair and Reconstruction. *Journal of bone and joint surgery. American volume* **95.** Place: United States Publisher: Copyright by The Journal of Bone and Joint Surgery, Incorporated, 2144–2151. ISSN: 0021-9355 (2013).
8. Uranues, S. *et al.* A New Synthetic Conduit for the Treatment of Peripheral Nerve Injuries. *World J Surg* **44,** 3373–3382. ISSN: 1432-2323 (Oct. 2020).
9. Bittner, G. D., Schallert, T. & Peduzzi, J. D. Degeneration, Trophic Interactions, and Repair of Severed Axons: A Reconsideration of Some Common Assumptions. *Neuroscientist* **6.** Publisher: SAGE Publications Inc STM, 88–109. ISSN: 1073-8584. https://doi.org/10.1177/107385840000600207 (2021) (Apr. 1, 2000).

10. Wagstaff, L. J. *et al.* Failures of nerve regeneration caused by aging or chronic denervation are rescued by restoring Schwann cell c-Jun. *Elife* **10,** e62232. ISSN: 2050-084X (Jan. 21, 2021).
11. Squintani, G. *et al.* Nerve regeneration across cryopreserved allografts from cadaveric donors: a novel approach for peripheral nerve reconstruction. *Journal of Neurosurgery* **119,** 907–913. ISSN: 0022-3085, 1933-0693. https://thejns.org/view/journals/j-neurosurg/119/4/article-p907.xml (2018) (Oct. 2013).
12. Pfister, B. J. *et al.* Biomedical engineering strategies for peripheral nerve repair: surgical applications, state of the art, and future challenges. *Crit Rev Biomed Eng* **39,** 81–124. ISSN: 0278-940X (2011).
13. Zilic, L. *Development of acellular porcine peripheral nerves* PhD thesis (University of Sheffield, Oct. 2016). https : / / etheses . whiterose . ac . uk / 15777/ (2021).
14. Evans, P. J. *et al.* Cold preserved nerve allografts: Changes in basement membrane, viability, immunogenicity, and regeneration. *Muscle & Nerve* **21.** eprint: https://onlinelibrary.wiley.com/doi/pdf/10.1002/%28SICI%291097-4598%28199811%2921%3A11%3C1507%3A%3AAID- MUS21%3E3.0.CO%3B2-W, 1507–1522. ISSN: 1097-4598. http : / / onlinelibrary . wiley . com / doi / abs / 10 . 1002 / %28SICI % 291097 - 4598 % 28199811 % 2921 % 3A11 % 3C1507 % 3A % 3AAID - MUS21%3E3.0.CO%3B2-W (2021) (1998).
15. Siemionow, M. & Brzezicki, G. in *International Review of Neurobiology* 141–172 (Academic Press, Jan. 1, 2009). https://www.sciencedirect.com/science/article/ pii/S0074774209870086 (2021).
16. Lanier, S. T., Jordan, S. W., Ko, J. H. & Dumanian, G. A. Targeted Muscle Reinnervation as a Solution for Nerve Pain. *Plastic and Reconstructive Surgery* **146,** 651e. ISSN: 0032-1052. https:// journals. lww. com/ plasreconsurg/ Fulltext/ 2020 / 11000 / Targeted Muscle Reinnervation as a Solution for. 48 . aspx (2021) (Nov. 2020).
17. Sunderland, S. The anatomy and physiology of nerve injury. *Muscle Nerve* **13,** 771–784. ISSN: 0148-639X (Sept. 1990).
18. Saffari, T. M., Bedar, M., Hundepool, C. A., Bishop, A. T. & Shin, A. Y. The role of vascularization in nerve regeneration of nerve graft. *Neural Regen Res* **15,** 1573–1579. ISSN: 1673-5374 (Sept. 2020).
19. Evans, P. J., Midha, R. & Mackinnon, S. E. The peripheral nerve allograft: A comprehensive review of regeneration and neuroimmunology. *Progress in Neurobiology* **43,** 187–233. ISSN: 0301-0082. https:// www. sciencedirect. com/ science/ article/ pii / 0301008294900019 (2021) (June 1, 1994).
20. Ide, C., Osawa, T. & Tohyama, K. Nerve regeneration through allogeneic nerve grafts, with special reference to the role of the schwann cell basal lamina. *Progress in Neurobiology* **34,** 1–38. ISSN: 0301-0082. https:// www. sciencedirect. com/ science/ article/ pii/ 030100829090024B (2021) (Jan. 1, 1990).
21. Cooper, D. K. C., Ezzelarab, M. B. & Hara, H. Low anti-pig antibody levels are key to the success of solid organ xenotransplantation: But is this sufficient? *Xenotransplantation* **24.** ISSN: 1399-3089 (2017).
22. Rutten, M. J., Janes, M. A., Chang, I. R., Gregory, C. R. & Gregory, K. W. Development of a Functional Schwann Cell Phenotype from Autologous Porcine Bone Marrow Mononuclear Cells for Nerve Repair. *Stem Cells Int* **2012,** 738484. ISSN: 1687-966X. https://www.ncbi.nlm.nih.gov/pmc/articles/PMC3388598/ (2021) (2012).
23. Hebebrand, D., Zohman, G. & Jones, N. F. Nerve Xenograft Transplantation: Immunosuppression with FK-506 and RS-61443. *Journal of Hand Surgery* **22,** 304–307. ISSN: 0266-7681. http : / / journals. sagepub. com / doi / 10 . 1016 / S0266 - 7681 % 2897 % 2980391 - 9 (2021) (June 1997).
24. Lin, S. S. *et al.* The role of natural anti-Gal alpha 1-3Gal antibodies in hyperacute rejection of pig-to-baboon cardiac xenotransplants. *Transpl. Immunol.* **5,** 212–218. ISSN: 0966-3274 (Sept. 1997).
25. Adigbli, G. *et al.* Humanization of Immunodeficient Animals for the Modeling of Transplantation, Graft Versus Host Disease, and Regenerative Medicine. *Transplantation* **104,** 2290–2306. ISSN: 1534-6080 (Nov. 2020).
26. Spitaleri, G. & Farrero, M. Translational Medicine in Brain Stem Death and Heart Transplantation. *Transplantation* **104,** 2258–2259. ISSN: 0041-1337. https : / / journals . lww . com / transplantjournal / Fulltext / 2020 / 11000 / Translational Medicine in Brain Stem Death and.11.aspx (2020) (Nov. 2020).
27. Burrell, J. C. *et al.* A Porcine Model of Peripheral Nerve Injury Enabling Ultra-Long Regenerative Distances: Surgical Approach, Recovery Kinetics, and Clinical Relevance. *bioRxiv,* 610147. https://www.biorxiv.org/content/10.1101/610147v1 (2019) (Apr. 16, 2019).
28. Lunney, J. K., Ho, C.-S., Wysocki, M. & Smith, D. M. Molecular genetics of the swine major histocompatbility complex, the SLA complex. *Developmental & Comparative Immunology* **33,** 362–374. ISSN: 0145305X. http : / / linkinghub. elsevier. com / retrieve / pii / S0145305X08001663 (2018) (Mar. 2009).
29. Denner, J. Paving the Path toward Porcine Organs for Transplantation. *New England Journal of Medicine* **377** (ed Phimister, E. G.) 1891–1893. ISSN: 0028-4793, 1533-4406. http:// www. nejm. org/ doi/ 10 . 1056 / NEJMcibr1710853 (2018) (Nov. 9, 2017).

30. Argaw, T., Colon-Moran, W. & Wilson, C. Susceptibility of porcine endogenous retrovirus to anti-retroviral inhibitors. *Xenotransplantation* **23,** 151–158. ISSN: 0908-665X. https:// www. ncbi. nlm. nih. gov/ pmc/ articles/ PMC4873160/ (2018) (Mar. 2016).
31. Demange, A. *et al.* Porcine endogenous retrovirus-A/C: biochemical properties of its integrase and susceptibility to raltegravir. *Journal of General Virology* **96,** 3124–3130 (2015).
32. Cowan, P. J. & Tector, A. J. The Resurgence of Xenotransplantation. *Am J Transplant* **17,** 2531–2536. ISSN: 16006135. http://doi.wiley.com/10.1111/ajt.14311 (2019) (Oct. 2017).
33. Fishman, J. A., Scobie, L. & Takeuchi, Y. Xenotransplantation-associated infectious risk: a WHO consultation: Xenotransplantation-associated infectious risk. *Xenotransplantation* **19,** 72–81. ISSN: 0908665X. http://doi.wiley.com/10.1111/j.1399-3089.2012.00693.x (2018) (Mar. 2012).
34. Chunasuwankul, R. *et al.* Low dose discontinued FK506 treatment enhances peripheral nerve regeneration. *Int Surg* **87,** 274–278. ISSN: 0020-8868 (Dec. 2002).
35. Wang, L. H. & Weiss, M. D. Anatomical, Clinical, and Electrodiagnostic Features of Radial Neuropathies. *Physical Medicine and Rehabilitation Clinics of North America. The Electrodiagnosis of Neuromuscular Disorders* **24,** 33–47. ISSN: 1047-9651. https://www.sciencedirect.com/science/article/pii/S1047965112000903 (2021) (Feb. 1, 2013).
36. Koo, B.-S. *et al.* Reference values of hematological and biochemical parameters in young-adult cynomolgus monkey (Macaca fascicularis) and rhesus monkey (Macaca mulatta) anesthetized with ketamine hydrochloride. *Laboratory Animal Research* **35,** 7. ISSN: 2233-7660. https://doi.org/10.1186/s42826-019-0006-0 (2021) (July 24, 2019).
37. Chen, Y. *et al.* Reference values of clinical chemistry and hematology parameters in rhesus monkeys (Macaca mulatta). *Xenotransplantation* **16.** eprint: https://onlinelibrary.wiley.com/doi/pdf/10.1111/j.1399-3089.2009.00554.x, 496–501. ISSN: 1399-3089. https://onlinelibrary.wiley.com/doi/abs/10.1111/j.1399-3089.2009.00554.x (2021) (2009).
38. *Tacrolimus (Oral Route) Proper Use - Mayo Clinic* https://www.mayoclinic.org/ drugs-supplements/tacrolimus-oral-route/proper-use/drg-20068314 (2021).
39. Chentanez, V., Cha-oumphol, P., Kaewsema, A., Agthong, S. & Huanmanop, T. Morphometric data of normal sural nerve in Thai adults. *J Med Assoc Thai* **89,** 670–674. ISSN: 0125-2208 (May 2006).
40. Ugrenovic´, S. *et al.* MORPHOLOGICAL AND MORPHOMETRIC ANALYSIS OF FASCICULAR STRUCTURE OF TIBIAL AND COMMON PERONEAL NERVES, 5.
41. Ugrenovic, S. Z., Jovanovic, I. D., Kovacevic, P., Petrovic´, S. & Simic, T. Similarities and dissimilarities of the blood supplies of the human sciatic, tibial, and common peroneal nerves. *Clinical Anatomy* **26.** eprint: https://onlinelibrary.wiley.com/doi/pdf/10.1002/ca.22135, 875–882. ISSN: 1098-2353. http : / / onlinelibrary. wiley. com/ doi/ abs / 10 . 1002 / ca. 22135 (2021) (2013).
42. Gustafson, K. J., Grinberg, Y., Joseph, S. & Triolo, R. J. Human distal sciatic nerve fascicular anatomy: Implications for ankle control using nerve-cuff electrodes. *Journal of Rehabilitation Research and Development* **49.** Num Pages: 13 Place: Washington, United States Publisher: Superintendent of Documents, 309-21. ISSN: 07487711. https : / / www. proquest . com / docview / 1013613406 / abstract / 62DF7E9D03024B7EPQ/1 (2021) (2012).
43. Zhang, Y. *et al.* A nerve graft constructed with xenogeneic acellular nerve matrix and autologous adipose-derived mesenchymal stem cells. *Biomaterials* **31,** 5312–5324. ISSN: 1878-5905 (July 2010).
44. Bhatheja, K. & Field, J. Schwann cells: Origins and role in axonal maintenance and regeneration. *The International Journal of Biochemistry & Cell Biology* **38,** 1995–1999. ISSN: 13572725. https:// linkinghub. elsevier. com/ retrieve/ pii / S1357272506001634 (2021) (Jan. 2006).
45. Hudson, T. W., Liu, S. Y. & Schmidt, C. E. Engineering an improved acellular nerve graft via optimized chemical processing. *Tissue Eng* **10,** 1346–1358. ISSN: 1076-3279 (Oct. 2004).
46. Whitlock, E. L. *et al.* Processed allografts and type I collagen conduits for repair of peripheral nerve gaps. *Muscle & Nerve* **39,** 787–799. ISSN: 1097-4598. http://onlinelibrary.wiley.com/doi/abs/10.1002/mus.21220 (2019) (2009).
47. Saheb-Al-Zamani, M. *et al.* Limited regeneration in long acellular nerve allografts is associated with increased Schwann cell senescence. *Exp Neurol* **247,** 165–177. ISSN: 1090-2430 (Sept. 2013).
48. Weber, R. A., Breidenbach, W. C., Brown, R. E., Jabaley, M. E. & Mass, D. P. A randomized prospective study of polyglycolic acid conduits for digital nerve reconstruction in humans. *Plast Reconstr Surg* **106,** 1036–1045, discussion 1046–1048. ISSN: 0032-1052 (Oct. 2000).
49. Zalewski, A. A. & Silvers, W. K. An evaluation of nerve repair with nerve allografts in normal and immunologically tolerant rats. *Journal of Neurosurgery* **52.** Publisher: Journal of Neurosurgery Publishing Group Section: Journal of Neurosurgery, 557–563. https://thejns-org.proxy1.library.jhu.edu/view/journals/j- neurosurg/52/4/article-p557.xml (2021) (Apr. 1, 1980).
50. Quintes, S., Goebbels, S., Saher, G., Schwab, M. H. & Nave, K.-A. Neuron-glia signaling and the protection of axon function by Schwann cells. *Journal of the Peripheral Nervous System* **15.** eprint: https://onlinelibrary.wiley.com/doi/pdf/10.1111/j.1529-

8027.2010.00247.x, 10–16. ISSN: 1529-8027. https://onlinelibrary.wiley.com/doi/abs/10.1111/j.1529-8027.2010.00247.x (2021) (2010).

51. Nave, K.-A. & Trapp, B. D. Axon-Glial Signaling and the Glial Support of Axon Function — Annual Review of Neuroscience. *Annual Reviews of Neuroscience* **31.** https://www-annualreviews-org.ezproxy.neu.edu/doi/10.1146/annurev.neuro. 30.051606.094309 (2021) (July 12, 2008).
52. Holzer, P. *et al.* Vital, Porcine, Gal-Knockout Skin Transplants Provide Efficacious Temporary Closure of Full-Thickness Wounds: Good Laboratory Practice-Compliant Studies in Nonhuman Primates. *J Burn Care Res* **41,** 229–240. ISSN: 1559-0488 (2020).
53. Kim, S. *et al.* Molecular and genetic regulation of pig pancreatic islet cell development. *Development* **147,** dev186213. ISSN: 0950-1991. https://doi.org/10.1242/dev.186213 (2021) (Mar. 30, 2020).
54. Marquet, F. *et al.* Pig Skin Includes Dendritic Cell Subsets Transcriptomically Related to Human CD1a and CD14 Dendritic Cells Presenting Different Migrating Behaviors and T Cell Activation Capacities. *The Journal of Immunology* **193.** Publisher: American Association of Immunologists Section: IMMUNE REGULATION, 5883–5893. ISSN: 0022-1767, 1550-6606. https://www.jimmunol.org/content/193/12/5883 (2021) (Dec. 15, 2014).
55. Scha¨ fer, A. *et al.* Porcine Invariant Natural Killer T Cells: Functional Profiling and Dynamics in Steady State and Viral Infections. *Frontiers in Immunology* **10,** 1380. ISSN: 1664-3224. https://www.frontiersin.org/article/10.3389/fimmu.2019.01380 (2021) (2019).
56. Hoffe, B. & Holahan, M. R. The Use of Pigs as a Translational Model for Studying Neurodegenerative Diseases. *Frontiers in Physiology* **10,** 838. ISSN: 1664-042X. https://www.frontiersin.org/article/10.3389/fphys.2019.00838 (2021) (2019).
57. Schumacher, J. M. *et al.* Transplantation of embryonic porcine mesencephalic tissue in patients with PD. *Neurology* **54.** Publisher: Wolters Kluwer Health, Inc. on behalf of the American Academy of Neurology Section: Articles, 1042–1050. ISSN: 0028-3878, 1526-632X. https://n.neurology.org/content/54/5/1042 (2020) (Mar. 14, 2000).
58. Isacson, O. *et al.* Cell implantation therapies for Parkinson's disease using neural stem, transgenic or xenogeneic donor cells. *Parkinsonism & Related Disorders* **7,** 205–212. ISSN: 13538020. https:// linkinghub. elsevier. com/ retrieve/ pii / S1353802000000596 (2021) (July 2001).
59. Chari, R. S. *et al.* Treatment of Hepatic Failure with ex Vivo Pig-Liver Perfusion Followed by Liver Transplantation. *New England Journal of Medicine* **331.** Publisher: Massachusetts Medical Society eprint: https://doi.org/10.1056/NEJM199407283310404, 234–237. ISSN: 0028-4793. https://doi.org/10.1056/NEJM199407283310404 (2021) (July 28, 1994).
60. Gold, B., Katoh, K. & Storm-Dickerson, T. The immunosuppressant FK506 increases the rate of axonal regeneration in rat sciatic nerve. *J. Neurosci.* **15,** 7509–7516. ISSN: 0270-6474, 1529-2401. https://www.jneurosci.org/lookup/doi/10.1523/JNEUROSCI.15-11-07509.1995 (2021) (Nov. 1, 1995).
61. Yang, R. K. *et al.* Dose-Dependent Effects of FK506 on Neuroregeneration in a Rat Model: *Plastic and Reconstructive Surgery* **112,** 1832–1840. ISSN: 0032- 1052. http://journals.lww.com/00006534-200312000-00012 (2020) (Dec. 2003).
62. Yan, Y., Sun, H. H., Hunter, D. A., Mackinnon, S. E. & Johnson, P. J. Efficacy of Short-Term FK506 Administration on Accelerating Nerve Regeneration. *Neurorehabil Neural Repair* **26.** Publisher: SAGE Publications Inc STM, 570–580. ISSN: 1545-9683. https://doi.org/10.1177/1545968311431965 (2021) (July 1, 2012).
63. Auba´, C., Hontanilla, B., Arcocha, J. & Gorr´ıa, O´ . Peripheral nerve regeneration through allografts compared with autografts in FK506-treated monkeys. *Journal of Neurosurgery* **105.** Publisher: American Association of Neurological Surgeons Section: Journal of Neurosurgery, 602–609. https://thejns-org.proxy1.library.jhu. edu/view/journals/j-neurosurg/105/4/article-p602.xml (2021) (Oct. 1, 2006).
64. Gold, B. G., Storm-Dickerson, T. & Austin, D. R. The immunosuppressant FK506 increases functional recovery and nerve regeneration following peripheral nerve injury. *Restor Neurol Neurosci* **6,** 287–296. ISSN: 0922-6028 (Jan. 1, 1994).
65. Wang, M. S., Zeleny-Pooley, M. & Gold, B. G. Comparative dose-dependence study of FK506 and cyclosporin A on the rate of axonal regeneration in the rat sciatic nerve. *J Pharmacol Exp Ther* **282,** 1084–1093. ISSN: 0022-3565 (Aug. 1997).
66. Kim, J.-M. *et al.* Long-term porcine islet graft survival in diabetic non-human primates treated with clinically available immunosuppressants. *Xenotransplantation* **n/a.** eprint: https://onlinelibrary.wiley.com/doi/pdf/10.1111/xen.12659, e12659. ISSN: 1399-3089. https://onlinelibrary.wiley.com/doi/abs/10.1111/xen.12659 (2020).
67. Matsumoto, S. & Shimoda, M. Current situation of clinical islet transplantation from allogeneic toward xenogeneic. *Journal of Diabetes* **n/a.** eprint: https://onlinelibrary.wiley.com/doi/pdf/10.1111/1753-0407.13041. ISSN: 1753-0407. http:// onlinelibrary. wiley. com/ doi/ abs/ 10 . 1111 / 1753 - 0407 . 13041 (2020).
68. Wynyard, S., Nathu, D., Garkavenko, O., Denner, J. & Elliott, R. Microbiological safety of the first clinical pig islet xenotransplantation trial in New Zealand. *Xenotransplantation* **21,** 309–323. ISSN: 0908665X. http://doi.wiley.com/10.1111/xen.12102 (2019) (July 2014).
69. Whitlock, E. L. *et al.* Dynamic Quantification of Host Schwann Cell Migration into Peripheral Nerve Allografts. *Exp Neurol* **225,** 310–319. ISSN: 0014-4886. https: //www.ncbi.nlm.nih.gov/pmc/articles/PMC2956413/ (2021) (Oct. 2010).

70. Holzer, P. W. *et al.* Immunological response in cynomolgus macaques to porcine α-1,3 galactosyltransferase knockout viable skin xenotransplants—A pre-clinical study. *Xenotransplantation* **n/a.** eprint: https://onlinelibrary.wiley.com/doi/pdf/10.1111/xen.12632, e12632. ISSN: 1399-3089. https://onlinelibrary.wiley.com/doi/abs/10.1111/xen.12632 (2020) (n/a Aug. 11, 2020).
71. Denner, J. Detection of cell-free pig DNA using integrated PERV sequences to monitor xenotransplant tissue damage and rejection. *Xenotransplantation* **28.** eprint: https://onlinelibrary.wiley.com/doi/pdf/10.1111/xen.12688, e12688. ISSN: 1399-3089. https://onlinelibrary.wiley.com/doi/abs/10.1111/xen.12688 (2021) (2021).
72. Denner, J. Why was PERV not transmitted during preclinical and clinical xenotransplantation trials and after inoculation of animals? *Retrovirology* **15,** 28. ISSN: 1742-4690. https://retrovirology.biomedcentral.com/articles/10.1186/s12977-018- 0411- 8 (2019) (Dec. 2018).
73. Althagafi, A. & Nadi, M. in *StatPearls* (StatPearls Publishing, Treasure Island (FL), 2021). http://www.ncbi.nlm.nih.gov/books/NBK549848/ (2021).
74. Arora, S., Goel, N., Cheema, G. S., Batra, S. & Maini, L. A Method to Localize The Radial Nerve Using the 'Apex Of Triceps Aponeurosis' as a Landmark. *Clin Orthop Relat Res* **469,** 2638–2644. ISSN: 0009-921X. https://www.ncbi.nlm.nih. gov/pmc/articles/PMC3148375/ (2021) (Sept. 2011).
75. Holzer, P. W. *et al.* A Comparative Examination of the Clinical Outcome and Histological Appearance of Cryopreserved and Fresh Split-Thickness Skin Grafts. *J Burn Care Res* **38,** e55–e61. ISSN: 1559-0488 (Feb. 2017).
76. Biomere. *PRT18-01 Neurography Audited Report* (Nov. 18, 2019).
77. Wang, D. *et al.* A simple model of radial nerve injury in the rhesus monkey to evaluate peripheral nerve repair. *Neural Regeneration Research* **9,** 1041. ISSN: 1673-5374. http://www.nrronline.org/text.asp?2014/9/10/1041/133166 (2018) (2014).
78. *Injury of Radial Nerve: Causes, Symptoms & Diagnosis* Healthline. https://www. healthline.com/health/radial-nerve-dysfunction (2021).
79. Gragossian, A. & Varacallo, M. in *StatPearls* (StatPearls Publishing, Treasure Island (FL), 2021). http://www.ncbi.nlm.nih.gov/books/NBK537304/ (2021).
80. Mohanna, P. N., Young, R. C., Wiberg, M. & Terenghi, G. A composite poly-hydroxybutyrate-glial growth factor conduit for long nerve gap repairs. *J Anat* **203,** 553–565. ISSN: 0021-8782 (Dec. 2003).
81. Scobie, L. *et al.* Long-Term IgG Response to Porcine Neu5Gc Antigens without Transmission of PERV in Burn Patients Treated with Porcine Skin Xenografts. *The Journal of Immunology* **191,** 2907–2915. ISSN: 0022-1767, 1550-6606. http: //www.jimmunol.org/cgi/doi/10.4049/jimmunol.1301195 (2018) (Sept. 15, 2013).
82. Tripathi, V. & Obermann, W. M. J. A Primate Specific Extra Domain in the Molecular Chaperone Hsp90. *PLOS ONE* **8.** Publisher: Public Library of Science, e71856. ISSN: 1932-6203. https:// journals. plos. org/ plosone/ article? id= 10 . 1371 / journal. pone. 0071856 (2021) (Aug. 9, 2013).

Table 1

Table 1 is available in the Supplementary Files section.

Figures

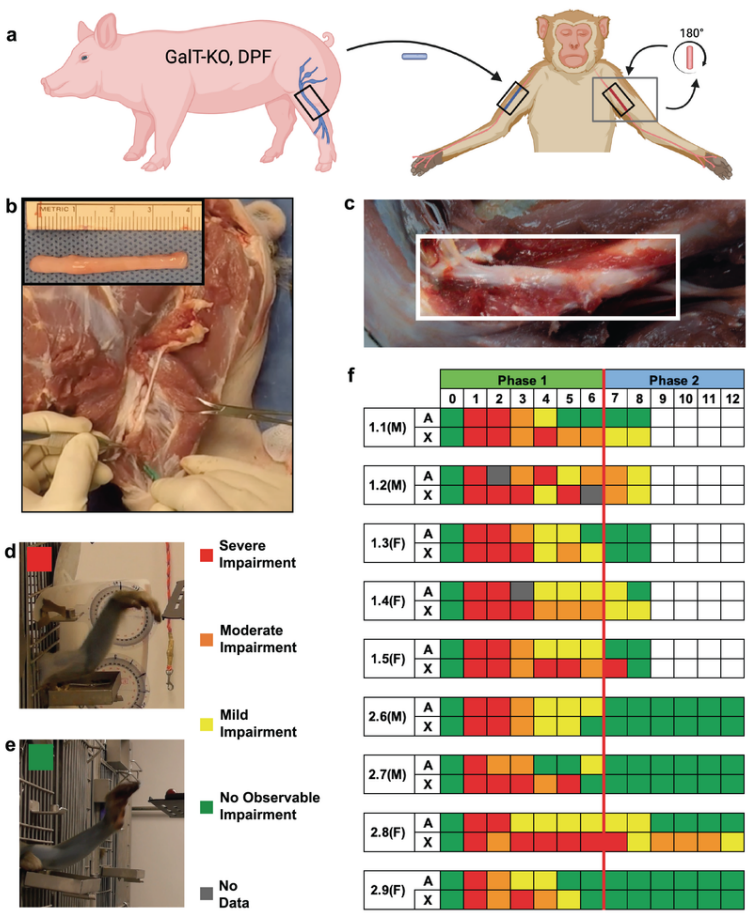

Figure 1

Experimental study design.

a, Schematic of experimental study design. Porcine sciatic nerve was trimmed to 4 cm and used to repair the complete transection of the radial nerve in 10 Rhesus Macaque recipients. In the contralateral arm, the transected, autologous radial nerve is rotated 180°and reimplanted as a control. **b**, Visualization of porcine sciatic nerve in situ during procurement surgery. Inset shows trimmed nerve (4 cm). **c**, Representative image of the reconstructed radial nerve from a limb treated with the xenogeneic transplant, photographed at necropsy (12- months postoperative). **d, e,** Recovery of wrist extension function was qualitatively assessed from monthly video recordings by an analyst blinded to the transplant type. Top image (d) depicts severe impairment, lower image (e) depicts no observable impairment. **f**, Magnitude of recovery of wrist extension function is illustrated via a heat map. Month 0 indicates baseline values for all graphs and heat maps. Phase 1 and 2 are separated by a line indicating variation in tacrolimus treatment. Numbers in the boxes to the left indicate specific subjects and their respective genders.

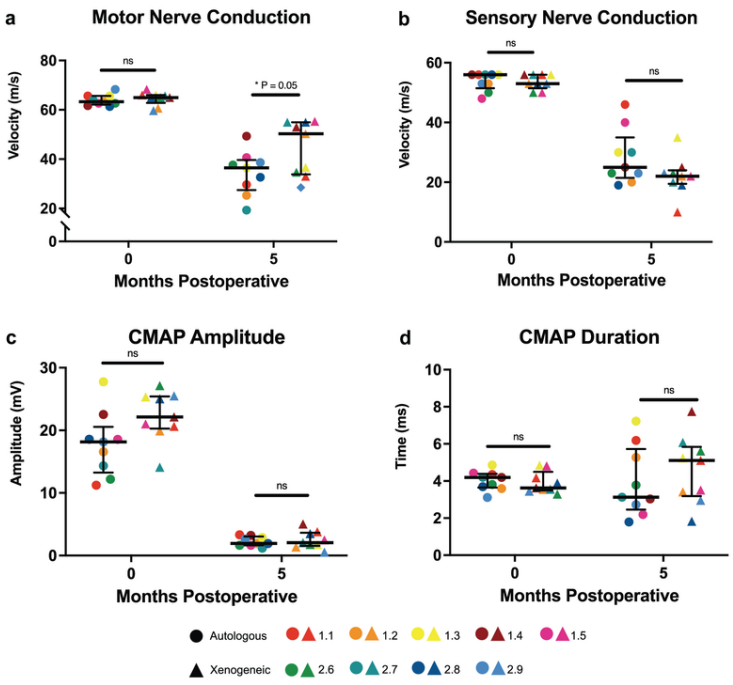

Figure 2

Phase 1 electrophysiological data.

All statistical analyses were performed using a Student's t-test; ns = not significant with a P≤0.05. **a**, Motor nerve conduction velocity showed partial recovery in all subjects, with the limbs treated with the xenogenic transplant exhibiting greater recovery.This was the only statistical difference in all of the electrophysiological data. **b**, Sensory nerve conduction velocity values were not statistically different, demonstrating only partial recovery compared to preoperative levels. **c**, At 5-months, compound muscle action potential (CMAP) amplitudes remained below the critical firing threshold in all limbs, and were statistically equivalent. **d**, CMAP duration values were varied between subjects, but combined, there was no statistical difference between the two transplant types.

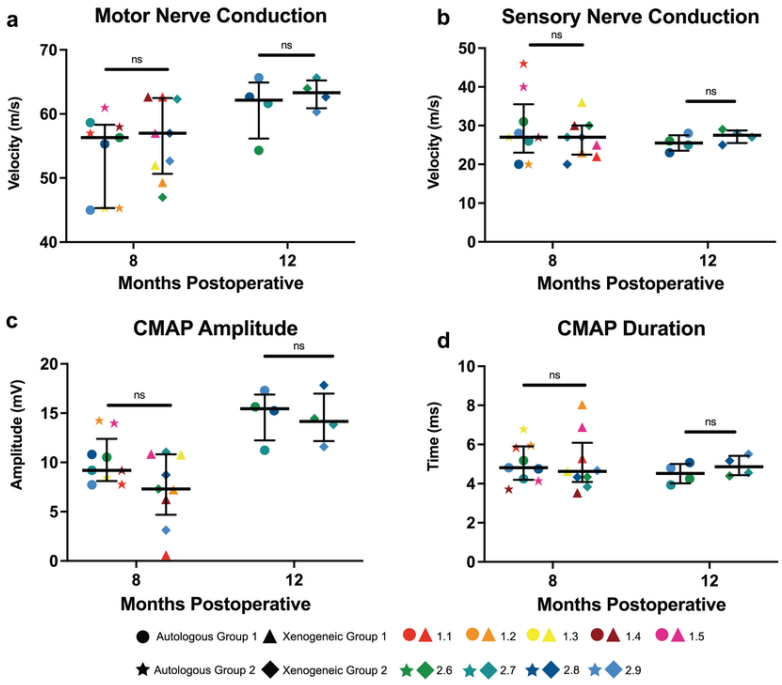

Figure 3

Phase 2 electrophysiological data.

All statistical analyses were done using a Student's t-test; ns = not significant with a P≤0.05. **a**, Motor nerve conduction velocities increased from Phase 1 values, and continued to increased between 8 and 12-months. There were no statistical differences in limbs treated with either transplant type. **b**, Sensory nerve conduction velocities increased from Phase 1, but appear to plateau at 8-months. **c**, Compound muscle action potential (CMAP) amplitudes increased significantly from 5-months, and continued to increase in magnitude by from 8 to 12-months approaching preoperative values, in all limbs regardless of transplant type. **d**, Negligible change in CMAP duration values occurred between 8 and 12 months, and were statistically equivalent between limbs treated with autologous or xenogeneic transplants.

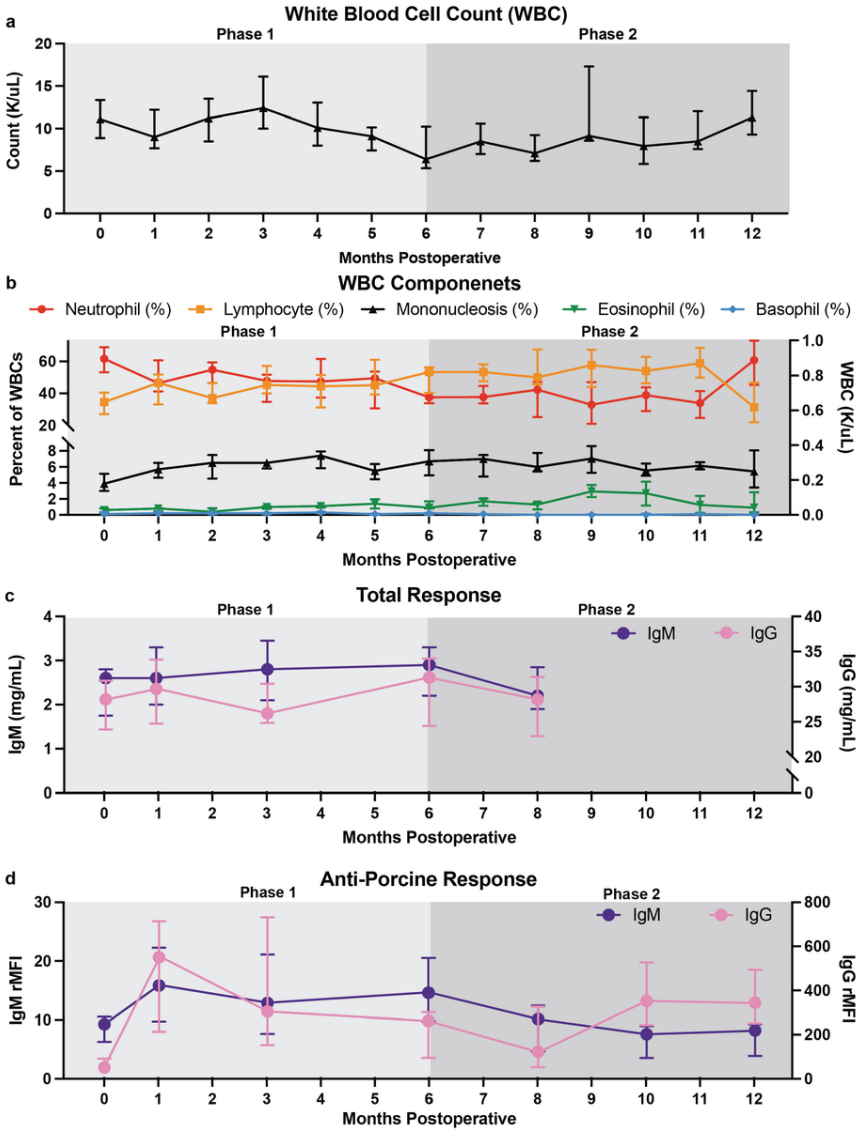

Figure 4

Immunogenicity following nerve reconstruction with xenogeneic nerve transplant.

a, Overall white blood cell count (WBC) remained at expected values for the entirety of the study. **b**, Composition of WBC populations remained within expected proportional ranges for the entirety of the study. **c**, Total IgM and IgG titer levels did not exceed variations of greater than +/-50% of baseline levels for all recipients over the course of the entire study. Data not available at 12-months for recipients in Group 2. **d**, Anti-Porcine IgM and IgG responses increased the greatest at 1-month postoperative, and demonstrated a gradual decrease by

8 and 12-months, respectively. Anti-porcine IgG levels remained elevated compared to preoperative levels.

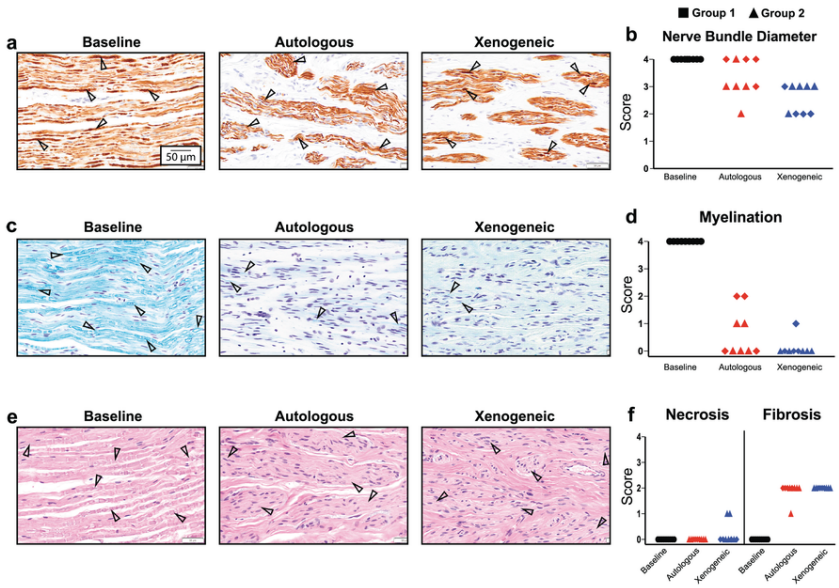

Figure 5

Histopathologic analysis of regenerated radial nerves.

a, Histology sections stained by immunohistochemistry for expression of neurofilament H. Arrowheads indicate axonal material. Representative images of native radial nerve at baseline, and explanted nerve samples obtained at necropsy from the regenerated nerve in both autologous and xenogeneic transplanted limbs. **b**, Nerve bundle diameters of the regenerated nerve from both transplant types were smaller than the diameters of native nerve obtained perioperatively, and qualitatively equivalent between the two transplant types. Higher scores indicate larger diameters. **c**, Luxol fast blue (LFB) staining was performed to assess the degree of myelination of regenerated nerve. Arrowheads indicate myelin. **d**, A reduction in the presence of myelin was observed in all regenerated nerves compared to baseline levels, favoring limbs treated with the autologous transplant. Higher score indicates greater presence of myelin. **e**, Necrosis and fibrosis were assessed using hematoxylin and eosin staining. Arrowheads indicate nerve bundles. **f**, Qualitative assessment of necrosis and fibrosis was equivalent in regenerated nerve tissue from both types of transplants. A higher score indicates greater degree of necrosis or fibrosis observed.

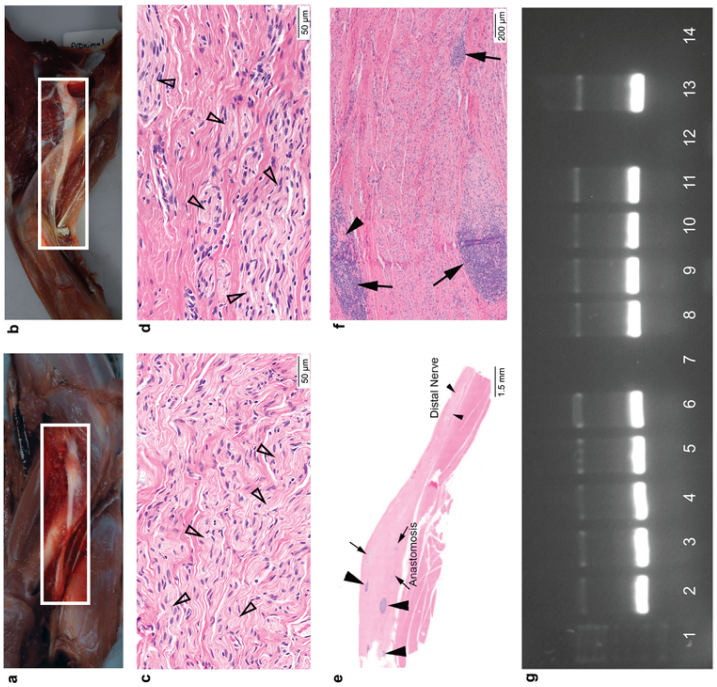

Figure 6

Cellular infiltrates, lymphoid follicles, and complete elimination of porcine material. a, Autologous treated limb at necropsy (12-months postoperative) demonstrating neuroma enlargment at anastomotic sites, expected as a result of the nerve repair surgery. **b**, Xenogeneic treated limb with similar presentation as seen in limbs treated with the autologous transplant. **c, d**, Representative histological images from sectioned regenerated nerve; left from autologous treated limb, xenogeneic on the right. Arrowheads indicate nerve bundles. **e**,**f** Low Power and High Power showing prominent tertiary lymphoid follicles, surrounding by cell populations of lymphocytes and macrophages infiltrating the regenerated nerve from a limb treated with the xenogeneic transplant. **g**, Qualitative PCR using primate-specific gene target demonstrates presence of primate cells and the absence of porcine cells at transplant sites repaired with autologous (lanes 2-6) and xenogeneic transplants (lanes 8-11). Lane 12 is the negative control, lane 13 is the primate control, and lane 14 is porcine control.

Supplementary Files

This is a list of supplementary files associated with this preprint. Click to download.

- Table1.pdf